Design and Development of a 6-Axis Robotic Manipulator for Paint Application

A Final Year Project Report

Presented to

School of Mechanical and Manufacturing Engineering (SMME)

Department of Mechanical Engineering

NUST

Islamabad, Pakistan

In partial fulfilment

Of the requirements for the degree of

Bachelors of Mechanical Engineering

By

Syed Muhammad Mustafa Kazmi

Zunairah Farooq

Danyal Ali

May 2019

EXAMINATION COMMITTEE

We hereby recommend that the Final Year Report Project prepared under our supervision by:

Syed Muhammad Mustafa Kazmi	00000123535
Zunairah Farooq	00000128228
Danyal Ali	00000130165

Titled: *"Design and Development of a 6-Axis Robotic Manipulator"* be accepted in partial fulfilment of the requirements for the award of Degree of Bachelors of Mechanical Engineering

Supervisor: Syed Hussain Imran, Dr.	_____ Dated
Committee Member: Amir Mubashir, Dr.	
Committee Member: Waqas Khalid, Dr.	

ABSTRACT

The automotive industry has manual painting operations involved in small scale industries particularly in under-developed countries like Pakistan. Automobile bodies, if painted manually, expose the paint workers to the chemicals present in the paint and increases their risk of developing respiratory tract cancers and other similar diseases. Manual paint application consumes more paint in comparison to an automated process for the paint application with the obvious reduction in the speed of the job. Our project is an industrial solution for the local automobile industries based in Pakistan which cannot afford expensive industrial robots to automate their manual processes like paint application of automobile parts and body. A 6-Axis articulated robot is capable of replacing the human workers in the paint application industries and enhance the speed while giving the optimal paint consumption during the process. Our robotic manipulator is a general-purpose prototype which can be used in paint application, welding, plasma cutting and process industry as a pick and place robot or by performing other specialized functions demanding high repeatability and speed. By changing the end-effector being used, the functionality of the manipulator can be changed easily. The design of the robot is basically inspired from KUKA-KR5 and FANUC-M10 series. A robotic arm can be made to follow certain trajectories with certain angular velocities, and can be controlled in a variety of ways.

ACKNOWLEDGEMENTS

We would like to express our deepest gratitude to our supervisor, Dr. Hussain Imran for his guidance throughout the project. We would also like to thank Dr. Mushtaq for his valuable advice when needed and Lecturer Hamza Asif Nizami for giving key insights during the design and fabrication phase. And to some fellow students for helping us selflessly through the most difficult times, they deserve due credit for their help. And to our parents, who put their trust in us and provided us with support; emotional and financial, and their pride in us enabled us to work with a sense of duty, the duty to return their trust with our untiring efforts and push our limits to achieve the goals we set for ourselves. And lastly, to NUST, for always providing us all possible resources to help us pursue our dreams and take pride in serving the people of this dear land.

We also place on record, a sense of gratitude to one and all, who directly or indirectly, have lent their hand in this venture.

ORIGINALITY REPORT

ORIGINALITY REPORT

7%	3%	3%	5%
SIMILARITY INDEX	INTERNET SOURCES	PUBLICATIONS	STUDENT PAPERS

PRIMARY SOURCES

1	Submitted to University of Reading Student Paper	<1%
2	Submitted to King's College Student Paper	<1%
3	www.docstoc.com Internet Source	<1%
4	"Intelligent Robotics and Applications", Springer Science and Business Media LLC, 2009 Publication	<1%
5	Submitted to Oxford Brookes University Student Paper	<1%
6	Submitted to Hariri Canadian University Student Paper	<1%
7	Biologically Inspired Control of Humanoid Robot Arms, 2016. Publication	<1%
8	Submitted to 7996 Student Paper	<1%

9	E BERNACKI. "Factors influencing the costs of workers' compensation", Clinics in Occupational and Environmental Medicine, 2004 Publication	<1%
10	Dasheek Naidu, Riaan Stopforth, Glen Bright, Shaniel Davrajh. "A Portable Passive Physiotherapeutic Exoskeleton", International Journal of Advanced Robotic Systems, 2017 Publication	<1%
11	Submitted to University of Wollongong Student Paper	<1%
12	Cihan Ayiz, Serdar Kucuk. "The kinematics of industrial robot manipulators based on the exponential rotational matrices", 2009 IEEE International Symposium on Industrial Electronics, 2009 Publication	<1%
13	docplayer.net Internet Source	<1%
14	Giancarlo Genta. "Introduction to the Mechanics of Space Robots", Springer Nature, 2012 Publication	<1%
15	Submitted to Nottingham Trent University Student Paper	<1%
16	Eduardo Salcedo, Dongcheon Baek, Aaron Berndt, Jong Eun Ryu. "Simulation and	<1%

	validation of three dimension functionally graded materials by material jetting", Additive Manufacturing, 2018 Publication	
17	www.greenseal.org Internet Source	<1%
18	Submitted to University of Portsmouth Student Paper	<1%
19	Submitted to Staffordshire University Student Paper	<1%
20	mars.uta.edu Internet Source	<1%
21	Submitted to Heriot-Watt University Student Paper	<1%
22	scholar.uwindsor.ca Internet Source	<1%
23	www4.comp.polyu.edu.hk Internet Source	<1%
24	Submitted to (school name not available) Student Paper	<1%
25	Submitted to University of Leeds Student Paper	<1%
26	Submitted to American University of the Middle East Student Paper	<1%

27	Submitted to University of Warwick Student Paper	<1%
28	Figueroa, Nadia B., Florian Schmidt, Haider Ali, and Nikolaos Mavridis. "Joint origin identification of articulated robots with marker-based multi-camera optical tracking systems", Robotics and Autonomous Systems, 2013. Publication	<1%
29	Submitted to University of Lancaster Student Paper	<1%
30	Submitted to Institute of Graduate Studies, UiTM Student Paper	<1%
31	Submitted to Higher Education Commission Pakistan Student Paper	<1%
32	www.engr.sjsu.edu Internet Source	<1%
33	S. Kim. "Efficient inverse kinematics for serial connections of serial and parallel manipulators", Proceedings of 1993 IEEE/RSJ International Conference on Intelligent Robots and Systems (IROS 93) IROS-93, 1993 Publication	<1%
34	www.scribd.com Internet Source	<1%

Exclude quotes	On	Exclude matches	Off
Exclude bibliography	On		

TABLE OF CONTENTS

LIST OF TABLES

LIST OF FIGURES

ABBREVIATIONS

KUKA- Keller und Knappich Ausburg

FANUC- Fuji Automatic Numerical Controls

ISO- International Organization for Standardization

IARC- International Agency for Research on Cancer

ABS- Acrylonitrile Butadiene Styrene

ABB- Asia Brown Boveri

SCARA- Selective Compliance Articulated Robot Arm

NEMA- National Electrical Manufacturer Association

NOMENCLATURE

T- Torque

FOS- Factor of Safety

ANSI – American National Standards Institute

CHAPTER 1: INTRODUCTION

Automotive paint industry involves manual painting of the vehicle body which dates back to more than 100 years. Painting of the vehicle body is a significant part of the overall manufacturing process and almost 40-50% of the total production cost is consumed on this part. The body was manually covered with a varnish like substance, then sanded and smoothed, followed by the reapplication of the varnish to hit a specific number of covering layers. The composition of the painting substance was volatile in nature in the beginning, which underwent a continuous improvement process in order to reduce the environmental hazards caused due to the chemicals present in the paint solution. But it only involved changes in the composition and types of the automotive paint to reduce the associated hazards and the drying time of the finished vehicle [1].

Since the advent of the industrial robots decades ago, automated painting of the body of a vehicle was initially one of the first jobs that we performed by the robots. In the beginning, hydraulic robots were introduced in the industry but they produced poor film builds and products of inferior quality and safety and while trying to improve the results being obtained by automating the process, the end result was an electronic manipulator that can easily replace the hydraulic robots in the industry [2]. But these industrial robots are quite big and expensive to be used in the industries and are only used in the larger industries.

Our project is to build a 6-Axis robotic manipulator for painting the auto-rickshaw bodies. This is an industrial solution for a local auto-rickshaws manufacturing industry, Sazgar Autos. A manipulator is the arm of the robot [3]. According to ISO,

"Manipulating industrial robot is an automatically controlled, reprogrammable, multi-purpose, manipulative machine with several degrees of freedom, which may be either fixed in place or mobile for use in industrial automation applications" [4]

The robot is easy to program and reprogram without any changes in its structural build depending on what job would be expected of the manipulator. Despite of all the aid that a robot provides in the industry, these manipulators are only there to take a bit of the job from humans and complete it with more perfection as compared to human workers because of the repeatability and consistency in their results and the manipulator, in no way, is going to completely eliminate the human resource in a particular work shop.

1.1 Motivation

The paint industries have had manual painting techniques until bigger industries started using industrial robots for various heavy duty jobs. The paint is actually a suspension of finely divided particles of pigment, thinner and a binder. The paint can either be acrylic or water or oil based [5]. The paint coated to the vehicle body generally is water-based and contains very minute amount of solvents but still are hazardous for the worker painting the body due to the presence of the volatile chemicals in the paint. Chemicals like toluene, xylene, esters, glycol ethers, ketones, alcohols and other aliphatic compounds which are volatile in nature cause cancers in the paint workers being exposed to paints occupationally. Most common types of cancers that caused casualties due to occupational exposures are lung cancer, mesothelioma and bladder cancer, childhood leukaemia due to maternal and paternal exposure, lympho-haematopoietic cancers and different chromosomal aberrations have been observed in the persons exposed to chemicals in the paint during painting operations [6].

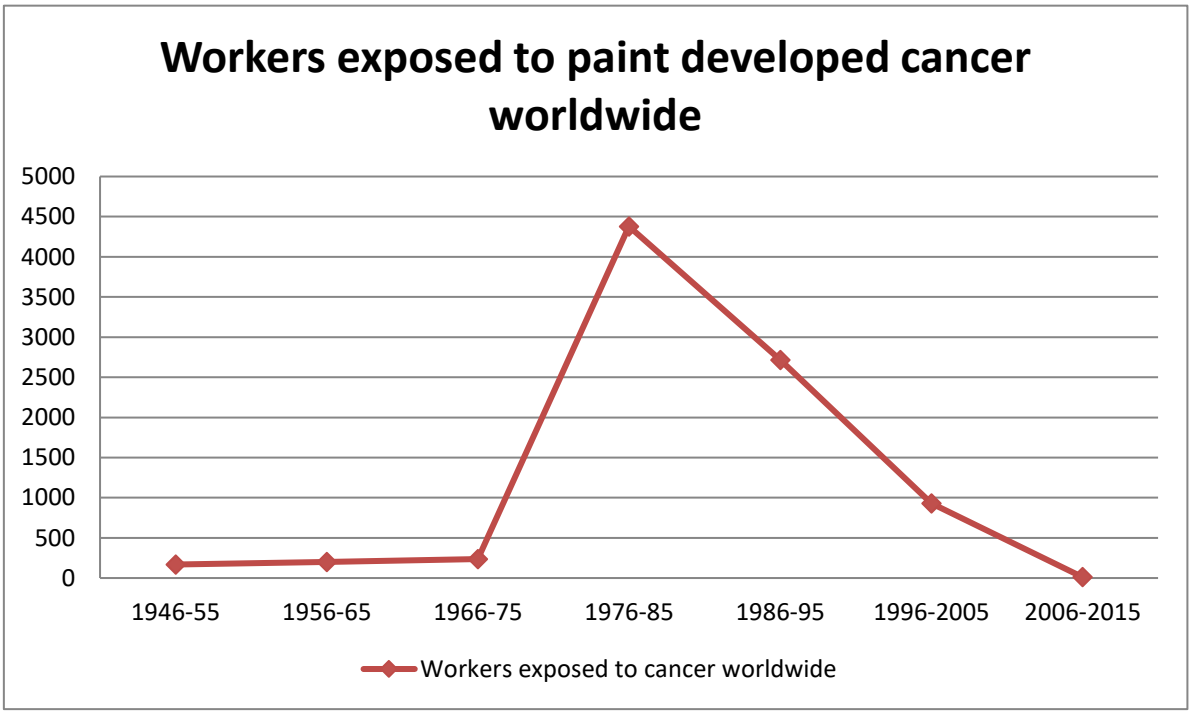

Figure 1: Data of industrial workers exposed to cancer worlwide across the years span mentioned

The trend shows the increase in the number of people exposed to cancer worldwide who work in the paint application industries and then a decrease due to the introduction of the concept of automation [6].

Automating the processes that involve dirty, dangerous and repetitive tasks requiring consistent precision and accuracy was the need of the time. Since manual paint application is not consistent and studies shows that paint is wasted during application by hand and about 15-30% wasted paint can be saved if the paint application processes are automated because in that way trigger accuracy and film thicknesses can be taken into account by simple repositioning of the end-effector [7]. Since the robot is programmed to do a particular job the output remains the same i.e. consistent and because the robot can work at a constant speed without any breaks in between the production, automation speeds up manufacturing.

Introducing automation in paint application industries would limit the safety hazards due to the toxicity of the paint but robot in no way can take over the whole of the job, it actually is the maintenance and calibration of the robot done by the human expertise which keep the process going, giving the maximum throughput all along [7].

1.2 Problem Statement

Design and development of a 6-Axis robotic manipulator to be used in paint application processes at Sazgar Autos.

1.3 Objectives

The deliverables of the project are:

- Complete design of the prototype
- Fabrication and assembly of the prototype
- Coding and testing of the prototype

CHAPTER 2: LITERATURE REVIEW

2.1 History of automation

Robotics was introduced to the industry in 1960's and the very initial tasks that were done by the robots included the application of paints [3]. In the beginning, the robots used to do the pick and place jobs in the industry. Later on, they developed more complex sensors and hence more complex trajectories and jobs became manageable for the industrial robots like welding, grinding etc. All industrial robots fall under any of the following three categories:

- Material handling robots
- Process operations robots
- Assembly robots

Material handling robots automate some of the tasks that are considered dull and tough, heavy-duty tasks, which if automated can easily eliminate the manpower in the industry against a safe investment. By material handling we mean various movements of the material on the floor such as,

- Part selection
- Part transfer
- Palletizing
- Packing
- Machine loading [9]

These robots simply exploit the capability of a robot to move around the floor and majority of the industrial robots belong to this category. These robots decrease the ergonomic hazards for the workers in the industry [10]. The trends in the ergonomics after automation in the manufacturing industries can be observed by the following graph [11].

Table 1: Injury and illness rates in manufacturing

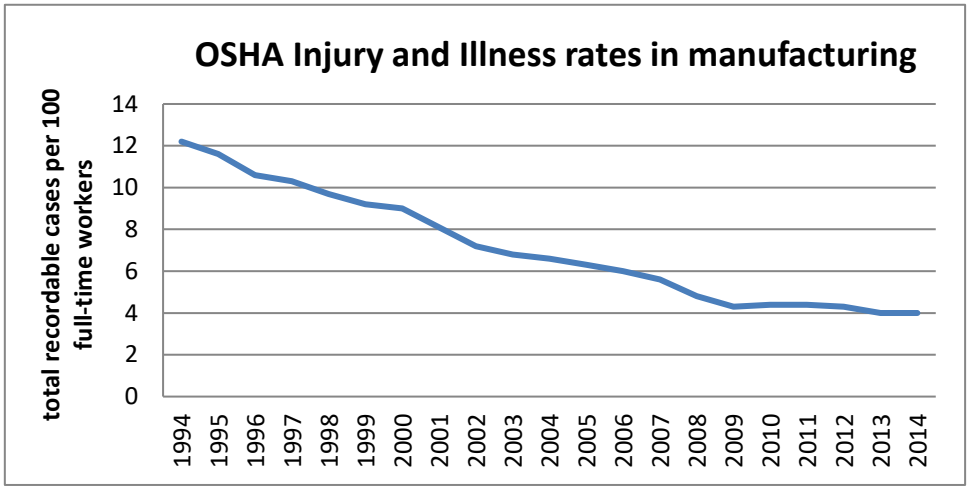

Process operations robots actually control the motion of their end-effector where some tool is fixed and they perform the job following the code fed in them. Our robot falls in this category too since its end-effector would be able to perform the paint application process in automotive industry.

Assembly robots are the robots used in lean manufacturing to increase the production speed and improve quality of the job. These are heavy duty robots used in only mega industries. Common industrial robots are [9]

- FANUC
- Yaskawa Motoman
- ABB
- KUKA
- Universal Robots

2.2 Types of robots

There are six basic types of robots [12] which are as follows:

- Cartesian
- Cylindrical
- SCARA
- Articulated
- Polar
- Delta

Cartesian robots are the simplest type of industrial robots and are preferred by majority of the industrial workers because of its simple programming. This robot can only traverse linear movements but these can be used to our advantage by making small changes in the configuration and structure but its large size is a disadvantage since it occupies a lot of space.

Cylindrical robots have a cylindrical shape of working space and can be placed easily in between the assembly lines. These robots are very simple in terms of pick and place job since it is a combination of rotational and linear actuators. It can pick material, rotate at any given angle and place the material in another assembly line. Its installation is not an issue but its applications are very limited.

SCARA robots are a combination of both the cartesian and cylindrical robots and contains all the six degrees of freedom, three translational and three rotational. These are very compact and efficient robots used in bio medical fields because of its accuracy and precision.

Articulated robots are the most preferred robots in terms of application because of their compactness and their capability to perform movements which other robots in the same available space cannot. Ours is an articulated robotic arm. It is a replica of human arm in an industry which enables it to exhibit movements like an arm.

Polar robots are the robots with sphere shaped work space and follow the polar trajectory which means one rotational degree of freedom and two translational degree of freedoms.

Delta robots are very delicate robots with intricate structures used in pharma industries. These have spider shaped structure and are not preferred in heavy industries due to its delicacy.

The articulated robots are used widely in industry now-a-days. They were introduced in the industry in late 1960's and were after that a major advancement in the technology used in the industry, and were basically a replacement to the human effort being put in different tasks. A major reason for the hit of the robots that they were cheap and did the job at hand at a low cost as compared to a human being. With the advancement in technology they were made flexible to settle in different work environments.

The robots are also useful in a work environment where the human safety during the performance of the task is at risk. Like fire-fighting and other similar applications in the industry like painting the cars. The use of robots became very wide in different parts of the

industry with the passage of time. In 1990 there half the robots in the industry as compared to 1998. In eight years the robots saw a new hype in their usage.

The mechanics and control of the manipulators in the working domain is carried out in different steps. Firstly we want to find out the location of different objects in space. For this we assign frames to the joints of different links. After assigning frames which describe the orientation and the location of each joint with respect to the previous joint and the base frame. This location is traced out using the D-H parameter convention.

After finding the position and orientation of each of the links and the joints we then move forward to find the relation between different link parameters and the final end-effectors position in 3-d space. The different link parameters that are used to get this final transformation include the link-length and link-offset and link-twist angles. This is done with the help of forward kinematics. In forward kinematics we define the position of the links along with the orientation in a transformation matrix and multiply these matrices to get the position of the end-effector along with the orientation w.r.t. base frame at the base of the robot.

The total number of degrees of freedom of the robot also possess an important role in describing the final orientation and position of the robot manipulator. In our case there six degrees of freedom that are utilized in finding out the final orientation and position of end-effector.

The next step after the forward kinematics of the robot is the use of inverse kinematics to find out the angles of different joints given the end-effectors position and orientation in space. In our problem the inverse kinematics has a key role to play while the robot in intended to move in space through the given path. During the motion of the tool of the robot follows a given path as suggested by the user. During motion through that path the robot traces the points along that path in given time. Using the values of that points along the path the robot calculates the angular rotation for each joint and updates its vale so that the joint turns and the combined movement of all joints make it possible for the end-effector to reach the desired location in 3-d space.

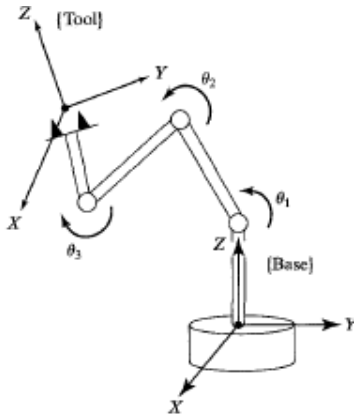

Figure 2: Simplified model of robot

During the motion of robot there are certain locations and the orientations of the robot that are not achievable by the robot and also there are certain positions at which the motion of different links does not affect the final position and orientation of the end-effector. The positions are the singularities. A robot arm must avoid these orientations to have a smooth motion along the described path. The singularities in the robot kinematics are avoided by describing the joint angles rotation limits that robot has to follow so that it does not fall into a singular position. To reach at any point in 3-d space three links are enough but with three links there are many possibilities of singular configurations. To reduce the singularities we had to include the redundant links which help in smooth and flexible motion of the robot end-effector.

After finding the angles through the inverse kinematics the next step is to find out the joint rates of all the joints that are given to the actuators to make them move. This is found out by the link parameters and finding the linear velocities of the links in terms of the angular velocities. Then in next step the angular velocities of all the joints are found in terms of the angular positions and the linear and angular velocities of the end-effector.

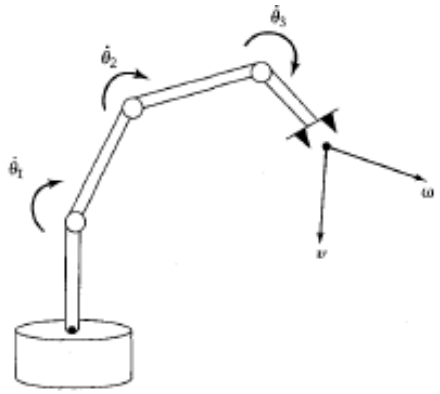

Figure 3: Simplified model of robot

Angular velocities of links ($\dot{\theta}_1\dot{\theta}_2\dot{\theta}_3$) in terms of the end-effector linear and angular velocities

Through the velocities relation we get the Jacobian which relates the linear and angular velocities of the end-effector w.r.t. the joint revolution rates. European and Japanese automotive industries have been using paint robots for coating interior as well as outer body parts of the car body [12]. Car interior, engine compartment, trunk, doors, door entries, interior parts of engine, rabbet, etc. are all painted by paint robots. Peugeot was the first company in Europe to use robot painting in its factories. Workspace of the robot is defined by the joint limits and the link lengths and the link configurations. It can be determined geometrically or also by the use of geometrical methods [13]. It does not include the end effector position, it only includes the links that are part of the robot body. Joint dependency and joint movements have to be studied to evaluate the functional workspace by the use of kinematic, geometric or analytical methods.

Joint limits are defined to prevent the robot from reaching singularity conditions and such configurations from which it is not possible for the robot to go back to its initial configuration. A detailed study of the joint configuration of industrial robots was done to understand the joint limits and configurations [14] [15].

The mechanical properties of ABS are determined by applying ISO standard and ASTM standard test methods. Finite Modelling and simulations are used to verify these tested values [16]. ABS is a thermoplastic that shows non-linear behaviour and the general true stress-true strain curves cannot be used to study the strength of ABS in structures. The curve starts deviating from the ideal behaviour and ends up showing limiting stress value which is less than the linear or ideal limit stress value. So, test methods enable the determination of properties which can be used in FEA software such as ANSYS and SolidWorks Simulation to perform stress analysis of any model made up of ABS or PC.

Robot motion cannot be studied unless kinematic equations are determined and solved for particular configurations and then verified. Before designing a robot, it is imperative that the existing robots kinematics be studied and experimented with. For this purpose, the kinematics of ABB IRB 140 was studied. Almaged [17] has presented kinematics analysis of the robot. Zennir [18] has studies the forward and inverse kinematics of Kawasaki Manipulator using SolidWorks and MATLAB SimMechanics. Singularities and inverse kinematics have been studied by Robert [19] and Rosheim [20] and they have presented closed form solution for the

manipulator wrist by creating conditions to avoid singularity conditions. Norbert and Adam [21] modelled 6 DOF manipulator in MATLAB and this contribution was studied to develop an understanding of the process of robot modelling in MATLAB environment. P Surendernath and K.Nagaraja Rao [22] have modelled a 6DOF robotic arm using SolidWorks and have also determined the joint torques. This contribution was studied to help develop an understanding of the modelling process.

CHAPTER 3: METHODOLOGY

4.1 Motor Selection

Stepper motors have been used for controlling the motion and rotation of the joints of our manipulator. Servo motors are considered the best to be used in the bots and the manipulators for its high speed and torque but since our job requires more holding torque and simpler commissioning with easy maintenance we went for the stepper motors to be used at our manipulator's joints [8]. Our manipulator is not expected to bear the dynamic loading and hence the edge the servo has over stepper gets nullified here. In fact, stepper motors are handy to use since these do not have encoders with them and hence are less complex and less expensive [8].

4.2 Motor Calculation

We have a total of 6 joints whose motion is to be controlled by six independent motors. The motors are to be installed on the joints and the specifications for those can be calculated theoretically for the maximum static loading which can be observed in fully-extended position. In torque calculations, both the inertial and rotational torques should be calculated and the sum of both of these determines the total torque according to which the motor is selected. Since the RPM required of the manipulator is very low and hence it makes the rotational torque for the shoulder joint that has the maximum weight and thus should give rise to the maximum torque gives the value

$$T = I\alpha = 0.0015 \text{ Nm}$$

This value does not make much difference to the inertial torque value and hence we can ignore calculating the rotational torque for every joint since it is going to make very small difference that too in the 10^{-3} decimal place. The calculation for the motors is started with the joint 6 and would go back to base joint i.e. joint 1. So that the additional weight on the previous joints because of the motors installed on the successive joints may be catered easily while calculating the loading conditions for all the joints.

Joint 6:

Joint 6 is the end-effector here which is holding the pencil in our prototype. The torque on the joint is only due to the weight of the pencil considered acting downwards in the extended position of the manipulator.

Mass of the pencil = m_p = 100g = 0.1kg

Length of the pencil = l_p = 18cm = 0.18m

Weight of the pencil = W_p = 0.1 x 9.81 = 0.981N

T_6 = 0.981 x 18 = 17.658Ncm = 0.17Nm

Joint 5:

Similarly, the torque on joint 5 is a sum of the torques due to the mass of the pencil at the end-effector and the motor (110g), the mass of the link 5 acting on its centre of mass. Hence,

T_5 = 0.145 + 0.182 = 0.327Nm

Joint 4:

The torque on joint 4 is the sum of the torques due to the weight of the link itself and the successive weights acting at their respective moment arms plus the weight of the motors at the two successive joints.

T_4 = 0.82Nm

Joint 3:

The torque on the fore-arm joint is the sum of all the torques due to the weight of the successive links and motors and the end effector present after this joint and the value is

T_3 = 3.76Nm

Joint 2:

The torque on the upper arm is the sum of all the links afterwards and the motors weight, acting vertically downwards at their respective moment arms and the value of torque is

T_2 = 12.6Nm

Joint 1:

The torque on the shoulder joint is equal to the torque due to the weights of the links of the manipulator and the motors, acting at their respective moment arms which give a total torque

T_1 = 20.52Nm

4.3 Selection of Material

For the structure to be light in weight, yet strong enough to support its own weight as well as the payload, a material has to be chosen that had sufficient yield strength and a certain degree of hardness. A comparison was performed between ABS plastic and Aluminum as the candidate materials for the prototype. After careful evaluation, Aluminum was selected. The cost of 3D printing ABS was too high and did not help us achieve the target of developing an affordable prototype. Moreover, observation of sample parts 3D printed from available facilities led to the conclusion that required profiles of the parts would be difficult to achieve , hence it was concluded that 3D printing the parts was not a viable option in this scenario. Analysis of the ABS model in simulation software showed a deflection of 8cm under the worst loading conditions, which meant that the structure would lose its integrity under loading conditions.

In light of the above observations, ABS was ruled out as a possible candidate and a decision was made to proceed with Aluminum as the material of choice given the intentions of developing a structurally stable, yet affordable prototype. Aluminum 6061 grade was chosen. 6061 is readily available in the local markets at a very affordable rate and it is easy to machine. Properties of the metal are shown in the appendix.

4.4 Design of the Manipulator

The design of the six axis robot manipulator required a thorough survey of the existing paint robots in the automotive industry. Well-renowned robot manufacturers such as FANUC, Universal Robots, KUKA and ABB provide a vast number of robot models to be used for various applications. Initially, the design of these models was studied and an understanding of the main design features was developed. In the automotive industry, robots used for painting purposes are almost always 6R robots, where all six joints are revolute and all joints rotate about their own axes and there is no translator motion in the joints. Such robots are capable of achieving almost all points within a nearly hemispherical region surrounding the robot, where the exception points are known as singularities. Finding these points which are not accessible by the robot is a tedious task. The workspace of the robot has to be contained within this hemisphere for the robot to be able to perform the desired functions to which it is programmed.

Some major features of the robot manipulator design include light and agile structure that does not fracture in operating conditions. After developing a good understanding of the major design features, the CAD design of the project was started in SolidWorks. For the development of the prototype, the dimensions were scaled down to achieve a working prototype at low cost.

A light design may be achieved in two ways; a hollow structure where possible and a less dense material that possess certain mechanical strength properties to ensure that it does not fail during operation. A lightweight design results in lesser stresses on the links and also ensures that torque on the motors remains within operating safety limits. The parts were modelled in SolidWorks and assembled together to form an assembly of the 6R robotic manipulator.

Motors are placed at the joints and sufficient space was provided at the joints to mount the geared motors using brackets.

4.5 Assembly

After modelling the parts, they were connected in an assembly, the standard views of which are shown below.

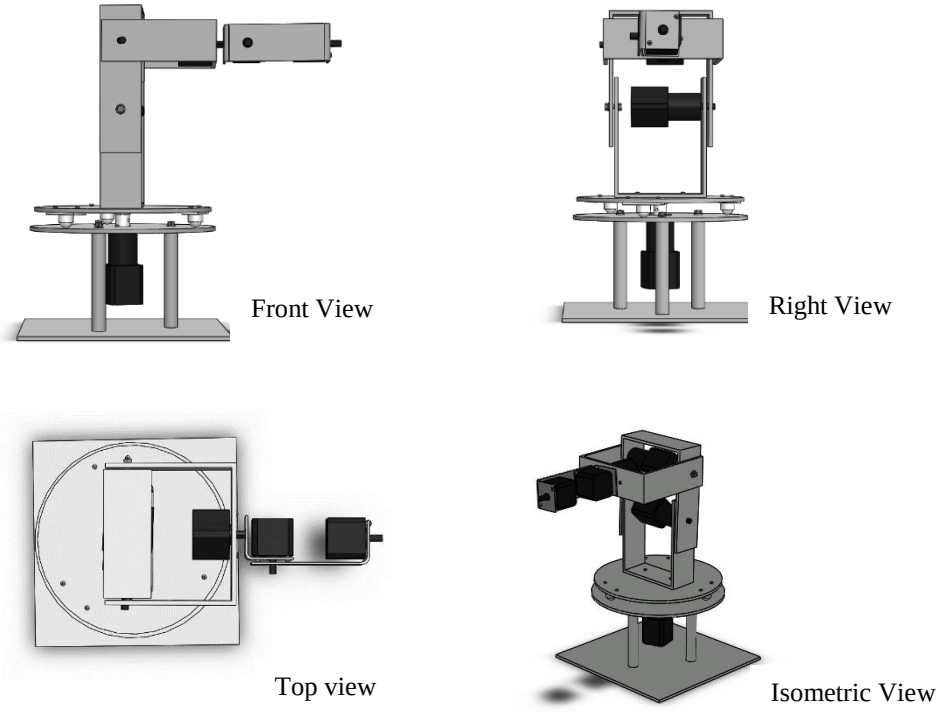

Figure 4: Standard views of the assembled robotic manipulator

4.6 Exploded View

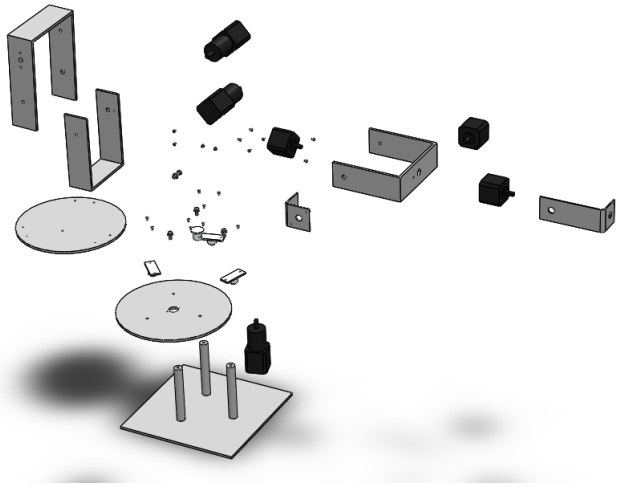

Figure 5: Exploded view of the six-axis robotic manipulator

4.7 Mass properties

The figure below shows the mass properties of the assembly obtained by assigning material to the assembly. The total mass of the assembly, the centres of masses of the links, and the moments of inertia are show for each link.

```
Mass properties of Static 1
    Configuration: Default
    Coordinate system: -- default --

Mass = 8369.79 grams

Volume = 1714741.06 cubic millimeters

Surface area = 591436.96  square millimeters

Center of mass: ( millimeters )
     X = 83.93
     Y = 249.63
     Z = 200.97

Principal axes of inertia and principal moments of inertia: ( grams *  square millimeters )
Taken at the center of mass.
      Ix = (-0.01,  0.97,  0.24)        Px = 58524123.52
      Iy = (-0.01, -0.24,  0.97)        Py = 181372679.72
      Iz = ( 1.00,  0.01,  0.01)        Pz = 192047580.76

Moments of inertia: ( grams *  square millimeters )
Taken at the center of mass and aligned with the output coordinate system.
     Lxx = 192032733.07          Lxy = -1322111.03          Lxz = -403967.84
     Lyx = -1322111.03           Lyy = 65458207.69          Lyz = 28321560.16
     Lzx = -403967.84            Lzy = 28321560.16          Lzz = 174453443.24

Moments of inertia: ( grams *  square millimeters )
Taken at the output coordinate system.
     Ixx = 1051635908.15         Ixy = 174043557.16         Ixz = 140781527.44
     Iyx = 174043557.16          Iyy = 462477255.37         Iyz = 448216549.45
     Izx = 140781527.44          Izy = 448216549.45         Izz = 754967478.59
```

Figure 6: Mass and inertia properties evaluated by SolidWorks

Joint limits were set after studying FANUC Mate 10 series and KUKA KR-5. In this assembly, the joint limits were set as follows

Table 2: Joint limits in assembly

Joint	Joint limit (^{0})
1	+170 to -170
2	+120 to -120
3	+120 to -120
4	+180 to -180
5	+120 to -120
6	+360 to -360

The above joint limits and the link lengths were used to define the workspace of the robot. The maximum horizontal reach of the robot was measured to be 33cm.

4.8 Structural Analysis

Structural analysis ensures that the design does not fail under working conditions. In a static analysis, all forces are considered to be constant throughout the analysis and these forces do no vary with time. In this case, there are no external forces acting on the robotic arm that are dependent on time so static structural analysis was used to check for the failure of the structure. Structural analysis was performed on SolidWorks Simulation. It was ensured that the maximum aspect ratio at any point in the assembly was not above 5, which is the convention in FEA for structural analysis. Mesh controls were applied to generate higher mesh density and restrict the mesh aspect ratio. Aspect Ratio (AR) is 1 for an ideal mesh where the element is a unilateral tetrahedral. AR was close to 1 for many locations in the assembly. External loads were applied in the form of gravity (9.81 m/s^2).

Large Displacement method was not used since no part in the assembly was to deflect significantly. LD method is used in cases such as when a flexible steel rod is wrapped around a rubber cylinder so it has to undergo a significant bending and deflection to achieve the desired end position. The convergence limit was set to 98%. For the non-linear analysis, multiple iterations were performed with respect to time and calculations were performed by SolidWorks

Simulation, and the solution was presented once the solution converged. Three types of solvers may be used in SolidWorks Simulation.

1. Direct Sparse Solver
2. FFE Plus
3. Large Problem Direct Sparse

Direct Sparse solver has more chances of convergence but i35t is limited by solution memory and often fails for larger assemblies. It is, however, fairly good at solving non-linear problems. FFE Plus is an iterative solution process which is less demanding on system memory and it is suitable for large problems. Large Problem Direct Sparse Solver is used for cases when Direct Sparse Solver runs short of memory. For this analysis, FFE Plus solver was used.

The mesh properties for the analysis were as follows:

Table 3: Mesh properties

Mesh type	Solid mesh
Mesher used	Curvature-based mesh
Jacobian points	4
Mesh control	Defined
Total nodes	100759
Total elements	51653
Max Aspect Ratio (AR)	4.934
Percentage of elements with AR < 3	99.3%

Table 4: Study properties

Analysis type	Non-linear static
Mesh type	Solid mesh
Large Displacement formulation	Off
Large Strain formulation	Off
Solver type	FFE Plus
Incompatible bonding options	Simplified

Control technique	Force
Iterative method	Newton-Raphson
Integration method	Newmark

4.9 Forward Kinematics

This robot is a 6 DOF (6R) robot. It includes 6 revolute joints connected at different offsets from previous joints. For solving and finding the kinematic equations of the robot, the first step was to find out the Denevit Hartenberg parameters of the robot. The D-H parameters are given as follows:

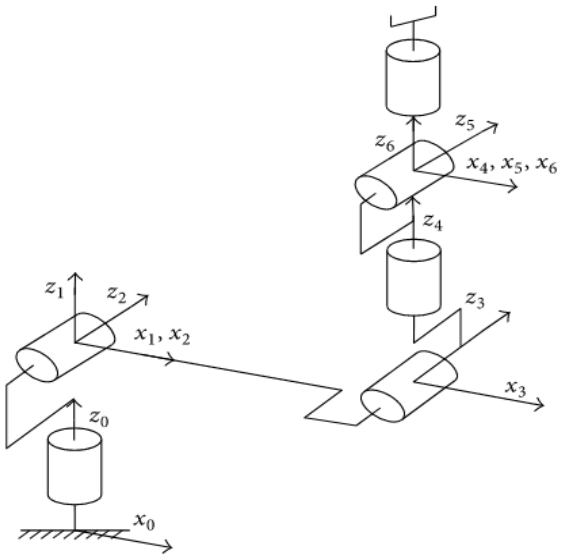

Figure 7: Kinematic structure of robot to determine DH parameters

Table 5: DH parameters from Kinematic model and robot dimensions

i	a_{i-1}	α_{i-1}	d_i	θ_i
1	13	+90	18	Θ1
2	38	0	0	Θ2
3	4.5	+90	-4	Θ3
4	0	-90	22	Θ4
5	0	+90	0	Θ5
6	0	0	12.75	Θ6

After finding the D-H parameters, the next step was to find the transformation matrices that give the orientation and position of each joint w.r.t. its previous joint. These matrices are multiplied to get the final transformation matrix of the end-effector w.r.t. the base.

$$T_{i-1}^{i} = R_x(\alpha_{i-1})D_x(a_{i-1})R_z(\theta_i)D_z(d_i)$$

$$T_{i-1}^{i} = \begin{bmatrix} \cos\theta_i & sin\theta_i & 0 & a_{i-1} \\ sin\theta_i cos\alpha_{i-1} & cos\theta_i cos\alpha_{i-1} & -sin\alpha_{i-1} & -sin\alpha_{i-1}d_i \\ sin\theta_i sin\alpha_{i-1} & cos\theta_i sin\alpha_{i-1} & cos\alpha_{i-1} & cos\alpha_{i-1}d_i \\ 0 & 0 & 0 & 1 \end{bmatrix}$$

$$T_1^0 = [cos(a) \ -sin(a)\ 0\ 150; 0\ 0\ -1\ 120;\ sin(a)\ cos(a)\ 0\ 0; 0\ 0\ 0\ 1];$$
$$T_2^1 = [cos(b) \ -sin(b)\ 0\ 350;\ sin(b)\ cos(b)\ 0\ 0;\ 0\ 0\ 1\ 0; 0\ 0\ 0\ 1];$$
$$T_3^2 = [cos(c) \ -sin(c)\ 0\ 65;\ 0\ 0\ -1\ 60;\ sin(c)\ cos(c)\ 0\ 0; 0\ 0\ 0\ 1];$$
$$T_4^3 = [cos(d) \ -sin(d)\ 0\ 0; 0\ 0\ 1\ 270;\ -sin(d)\ -cos(d)\ 0\ 0;\ 0\ 0\ 0\ 1];$$
$$T_5^4 = [cos(e) \ -sin(e)\ 0\ 0;\ 0\ 0\ -1\ 0;\ sin(e)\ cos(e)\ 0\ 0\ ; 0\ 0\ 0\ 1];$$
$$T_6^5 = [cos(f) \ -sin(f)\ 0\ 0;\ sin(f)\ cos(f)\ 0\ 0;\ 0\ 0\ 1\ 100; 0\ 0\ 0\ 1];$$

The final transformation matrix is given as:

$$T_6^0 = \begin{bmatrix} r11 & r12 & r13 & x \\ r21 & r22 & r23 & y \\ r31 & r32 & r33 & z \\ 0 & 0 & 0 & 1 \end{bmatrix}$$

From MATLAB the final X, Y and Z positions of the end-effector were found to be

$$X = f(\theta_1, \theta_2, \theta_3, \theta_4, \theta_5, \theta_6)$$
$$Y = f(\theta_1, \theta_2, \theta_3, \theta_4, \theta_5, \theta_6)$$
$$Z = f(\theta_1, \theta_2, \theta_3, \theta_4, \theta_5, \theta_6)$$

4.10 Inverse Kinematics

After finding the position and orientation of the robot the next task was to find the inverse kinematics of the robot where we can find the orientation of different links of the robot given the end effector position and pose. The inverse kinematics was done by splitting the robot into two halves. The first three joints were considered to find the position only of the end-effector while the last three joints were considered to intersecting at a point so they were only contributing to the orientation of the end-effector.

After doing the inverse kinematics we get the angular velocities of joints in terms of final position and orientation of the robot, which is same as we go from task space to the joint space. These inverse kinematic equations are used by the robot to follow the trajectory defined by the user. In doing inverse kinematics, the solution was obtained using the technique where only the first three of the joints determine the final position of the robot while the rest of three joints which are the last ones are considered to contribute only in the final orientation of the robot.

The method used to do the inverse kinematics is given as follows:

From the forward kinematics we had the final position as

X= $f(\theta_{1\to6})$

$$Y = f(\theta_{1\to6})$$

$$Z = f(\theta_{1\to6})$$

Also the orientation of the robot was defined as

$$R_6^0 = \begin{bmatrix} r_{11} & r_{12} & r_{13} \\ r_{21} & r_{22} & r_{23} \\ r_{31} & r_{32} & r_{33} \end{bmatrix}$$

- For the first three angles: $\theta_1, \theta_2, \theta_3$

We used the T_4^0 transform to define the position of the third links end point "A" with respect to base frame.

By getting the position of point A we got the first three angles by solving these equations

$$P_{Ax} = f(\theta_{1\to3})$$

$$P_{Ay} = f(\theta_{1\to3})$$

$$P_{Az} = f(\theta_{1\to3})$$

From these equations we get the first three angles for the given position of the end-effector.

- For finding the next three angles : $\theta_4, \theta_5, \theta_6$

We use the rotation matrix involved in the final orientation matrix along with the orientation matrix of end point with respect to the end-point of fourth link.

$$R_6^3 = R_4^3 R_5^4 R_6^5 = \begin{bmatrix} r_{11} & r_{12} & r_{13} \\ r_{21} & r_{22} & r_{23} \\ r_{31} & r_{32} & r_{33} \end{bmatrix}$$

From this rotation matrix the final three angles can also be obtained, for the given orientation specified by the user.

4.11 Angular velocities

After finding the inverse kinematics of the robot we moved onto finding the joint angular velocities which are the function of the end-effector linear and angular velocities. These two velocities are related through Jacobian using following relation.

$$\begin{bmatrix}\theta_1\\ \theta_2\\ \theta_3\\ \theta_4\\ \theta_5\\ \theta_6\end{bmatrix} = J^{-1}(\theta)\begin{bmatrix}\dot{X}_d\\ \dot{Y}_d\\ \dot{Z}_d\\ \omega_x\\ \omega_y\\ \omega_z\end{bmatrix}$$

$$J^{-1}(\theta) = \begin{bmatrix}J_{11}\,J_{12}\,J_{13}\,J_{14}\,J_{15}\,J_{16}\\ J_{21}\,J_{22}\,J_{23}\,J_{24}\,J_{25}\,J_{26}\\ J_{31}\,J_{32}\,J_{33}\,J_{34}\,J_{35}\,J_{36}\\ J_{41}\,J_{42}\,J_{43}\,J_{44}\,J_{45}\,J_{46}\\ J_{51}\,J_{52}\,J_{53}\,J_{54}\,J_{55}\,J_{56}\\ J_{61}\,J_{62}\,J_{63}\,J_{64}\,J_{65}\,J_{66}\end{bmatrix}$$

Where: $J_{11} = f(\theta_{1\to6})$

Similarly,$J_{21} = f(\theta_{1\to6})$

$$J_{31} = f(\theta_{1\to6})$$

..

..

$$J_{66=} f(\theta_{1\to6})$$

Also there are three components of end-effector velocities which are given by the derivatives of the parametric equations of the path. Our path equations are:

$$X_d = \cos(t)$$

$$Y_d = \sin(t) + 2$$

$$Z_d = 5(t)$$

Taking derivative of these parametric equations and substituting them into the angular velocity equation we can get the equations for angular velocities as

$$\dot{X}_d, \dot{Y}_d, \dot{Z}_d$$

Which are the linear velocities of the end-effector as a function of time along the path it has to follow as specified by the user.

3.12 Electronic components

To operate the robot, the electronic circuitry has to be established. In this robot, the control of the robot is delegated to two independent Arduino Uno, connected in parallel to the power supply. One Arduino board controls the three geared motors, i.e. the motion of the arm, and the second Arduino controls the movement of the wrist, which is operated by the motors at the joints fourth to sixth.

Stepper motors cannot be directly operated by a power source. A "driver" has to be connected to the motors and the Arduino. Stepper drivers operate by sending pulses to the motor. Drivers are of four types; one-phase, two-phase, one-two-phase and micro-stepping drivers. In this project, six DRV8825 were used. DRV 8825 is a micro-stepping driver. Such drivers deliver very smooth motion by increasing and decreasing current along a sine wave, so no pole is fully turned on or off. DRV 8825 is a 32X micro-stepping driver which divides each step of the stepper motor into further 32 discrete steps. Hence, one complete rotation of the motor shaft can be discretely divided into 11,520 steps in case of a gearless stepper motor. In case of the 100:1 geared steppers, the step size is 0.018 degrees, and after resolution into further discrete steps, the total resolution becomes 640,000 discrete steps. Such a high resolution enables the robot arm to move smoothly and without any apparent jerks or stutters. This smooth motion allows for consistent paint application and also reduces the structural vibrations.

The total current rating for the robot arm is as follows:

$$I = S_1 + S_2 + S_3 + s_4 + s_5 + s_6$$

where the capital notation is used for the geared motors and the lowercase notation is used for the gearless motors.

$$I = 1.68 + 1.68 + 1.68 + 1.68 + 1.68 + 1.68$$

$$I = 8.4\ amperes$$

In addition to this current, the two Arduino Uno and the drivers also draw current approximately equal to 1.5A. Taking into account the resistance of the wires and the low quality of the components circuitry in the local markets, more current is drawn by the components collectively, significantly more than the calculated current. Hence, a larger power supply was needed and it was decided to purchase a 16A, 12V fixed power supply with safety tripping. Connecting the circuit, the power supply was able to provide enough power to the robot to be able to run all six axes simultaneously.

3.13 Control System

Two methods to control the robot have been installed.

a) Pre-programmed trajectory fed into the microcontrollers allows the robot to move in an independent manner
b) A manual joystick control consisting of three joysticks, each joystick featuring the control of two axes, which enables the user to control the motion of all sixes axes at will

The algorithm was developed for the robot to follow an "S" trajectory. Angular velocities of all six motors were calculated and controlled during development of the algorithm to ensure that the robot follows the path without imminent stutters. A code was written in C++ for Arduino. A program was fed into the microcontroller to make the robot end-effector follow an "S-Trajectory" as the first control mechanism. The high resolution allowed for smooth, controlled motion of the arm. With minor changes, the robot can be programmed to follow any trajectory in its workspace, with spans a sphere of radius 33cm.

The joystick control gives a more hands-on control to the user and can be utilized in industrial applications such as in warehouses to manually control robots to lift and pick and place storage material. The angular velocities of the motors were controlled by controlling the pulses through

the driver. Hence, the robot can be made to move quickly, or in a more composed, slower manner, depending upon the nature of the application.

3.14 Cooling System

A fan was also installed for cooling the stepper drivers since they gained excessive heat owing to the passage of nearly 2A current through each driver. The fan was rated for 0.15A current and operated at 12V fixed DC voltage. Fins were also attached on top of the drivers to help preserve the integrity of the driver circuit. Upon operating the robot continuously for 30 minutes, no damage was recorded to the drivers, demonstrating the effectiveness of the cooling system thus installed.

CHAPTER 4: RESULTS AND DISCUSSIONS

5.1 Motors

From the methodology followed, the torques at the joints were calculated by catering for the static torque, which is due to the weights acting and their respective moment arms, and the torque due to the angular acceleration of the links.

Table 6: Joint torques of the robot arm and the selected motors

Joint	Joint torque	Motor
1	20.52	NEMA-17 100:1
2	12.6	NEMA-17 100:1
3	3.76	NEMA-17 100:1
4	0.82	NEMA-17
5	0.327	NEMA-17
6	0.17	NEMA-17

These results were used to determine the motors that are to be used at the joints. Motor selection required analysing the torque-omega curves of stepper motors. Since the torques are higher at the base and shoulder (joints 1 and 2), the stepper motors to be used here need to have speed reduction to increase the torque output of the motors. Based on market analysis, the motors were selected as shown in the table above. The speed needs to be reduced to increase torque. The following curve for NEMA-17 shows the torque output at varying motor rpm.

NEMA-17 gives approximately 0.44N.m torque at 500rpm if the motor does not apply gear reduction. If we use a planetary gear reducer of 100:1, the torque increases to 26.44N.m. The maximum torque encountered at the base joint is 20.52N.m and this geared motor provides a torque of 26.44N.m which is sufficiently greater. This tolerance accounts for friction effects and power losses in the actual model. Similarly, the calculation for the subsequent motors were performed and speed reducers were selected for each motor, if needed. The last motor which moves the end effector only has to move the weight of the end effector, so there is not much torque acting at this joint. Hence, a geared motor is not needed here and only a simple stepper motor performs the needed function here.

The characteristic curve of selected motors follows:

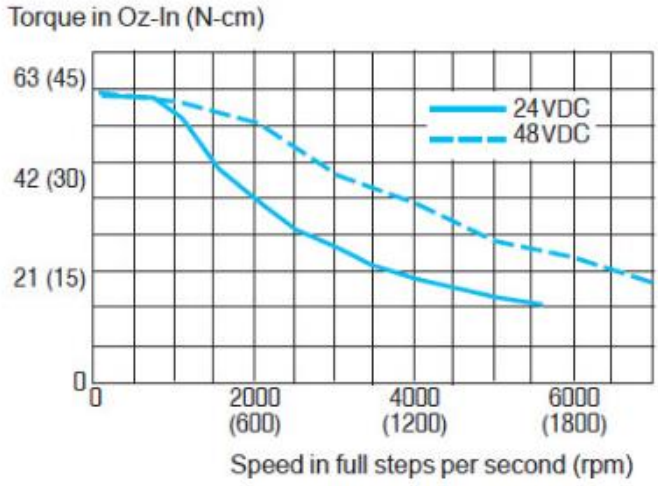

Figure 8: Characteristic curve of NEMA-17 Stepper motor [25]

5.2 Structural Analysis

Static analysis was performed which produced the results under specified conditions of fixtures and loads. The structure remained intact and the material did not yield in the worst case scenario, which concludes that the structure will not fail under ordinary working conditions.

The maximum stress in the design is 2.36MPa which does not exceed the ultimate strength of Al 6061 which is 55.14MPa. The von Mises stress is used to predict the maximum stress the structure faces and this value is compared with the Yield strength of the robot, after which the robot might become permanently deformed, but such a condition is not reached even in the most critical position of the robot. So, it can safely be deduced that the robot does not fail. Furthermore, the strain in the design is minimal, the figure that follows shows the equivalent strain plot of the assembly.

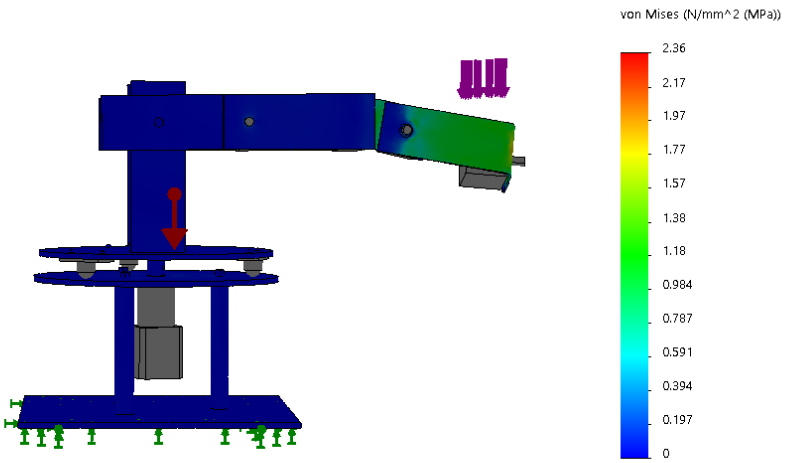

Figure 9: Stress analysis shows the maximum stress well below yield point

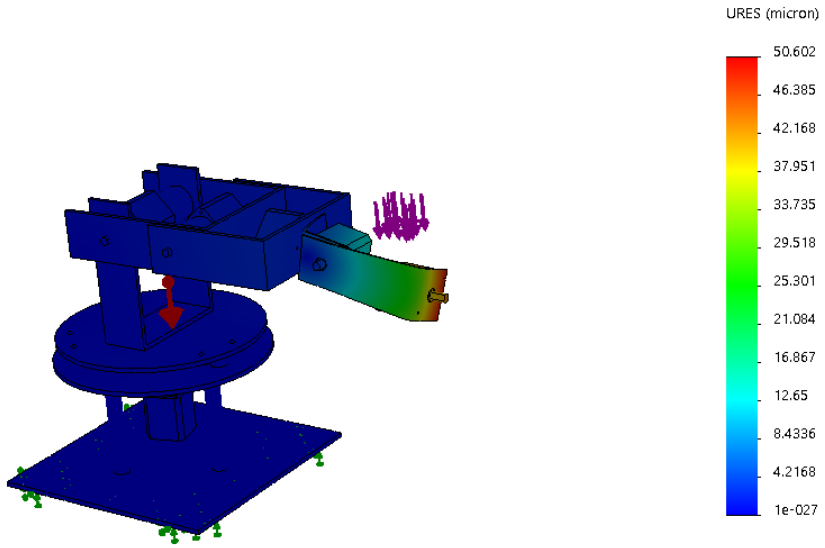

Figure 10: Simulation results show a negligible deflection under loading conditions

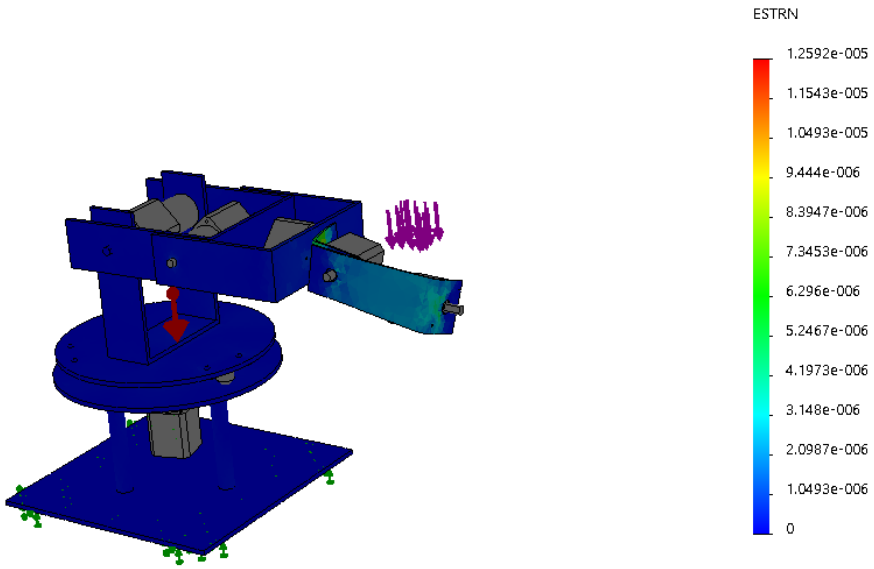

Figure 11: Simulation results show a negligible strain under loading conditions

5.3 Forward and Inverse Kinematics

By using the D-H parameter convention the position of the end-effector of robot is obtained in terms of the joint rotation of the all the joints. The X, Y and Z position of the end-effector is:

$$X=(9*cos(a+b))/2+38*cos(a)+(51*cos(a+b)*sin(c+d))/8-22*cos(a+b)*sin(c)+(51*sin(a+b)*cos(d))/4-(51*cos(a+b)*sin(c-d))/8+13$$

$$Y=-22*cos(c)-(51*sin(c)*sin(d))/4-18$$

$$Z=(9*sin(a+b))/2+38*sin(a)+(51*sin(a+b)*sin(c+d))/8-(51*cos(a+b)*cos(d))/4-22*sin(a+b)*sin(c)-(51*sin(a+b)*sin(c-d))/8$$

Where a, b, c, d, e and f represent the 6 angles of all the joints.

The forward kinematics of the robot was verified from the robotics toolbox in MATLAB by entering the angles to the joints through which they have moved. The final position of the robot through our forward kinematics equations and from the robotics toolbox was found to be in line and match with each other. After the forward kinematics the inverse kinematics of the robot was verified by substituting the final position in equations for angles and we get the angles to be same as we entered earlier in forward kinematics.

$$\theta_1 = Atan2(P_{xa}, P_{ya}) - Atan2(d_3, \pm\sqrt{(P^2{}_{ax} + P^2{}_{ay} - d^2{}_3)})$$

$$\theta_2 = Atan2((P_{xa}C_1, P_{ya}S_1 - a_1), P_{az}) - Atan2((P_{xa}C_1, P_{ya}S_1 - a_1)^2, P_{az}{}^2 - t_1{}^2)$$

$$\theta_3 = Atan2((P_{xa}C_1 + P_{ya}S_1 - a_1 - a_2C_2), P_{az} + a_2S_2) - \theta_2$$

The last three angles of the joints determine only the orientation of the end-effector and they are determined from the rotation matrix of the last end-effector with respect to the 3 frame.

$$\theta_5 = Atan2(\pm\sqrt{(a_{wx}{}^2 + a_{wy}{}^2)}, a_{wz})$$

$$\theta_4 = Atan2\left(\frac{a_{wy}}{s_5}, \frac{a_{wx}}{s_5}\right)$$

$$\theta_6 = Atan2\left(\frac{m_{wy}}{s_5}, \frac{m_{wx}}{s_5}\right)$$

Using these equations the inverse kinematics of the robot was verified from the robotics toolbox in MATLAB. After finding the inverse kinematics the velocities of the joint/ motors were determined with the help of the Jacobian relation in MATLAB. This code can be found in the appendix [17].

Where,

$$\begin{bmatrix}\theta_1\\ \theta_2\\ \theta_3\\ \theta_4\\ \theta_5\\ \theta_6\end{bmatrix} = J^{-1}(\theta)\begin{bmatrix}\dot{X}_d\\ \dot{Y}_d\\ \dot{Z}_d\\ \omega_x\\ \omega_y\\ \omega_z\end{bmatrix}$$

CHAPTER 5: CONCLUSION AND RECOMMENDATIONS

6.1 Conclusions

A detailed structural analysis of the robot was done and the applied conditions show that the structure does not fail. Motors were selected by calculating torques at joints and then speed reduction was performed by using additional gear drives for the motors to achieve a torque greater than that encountered at the joints. A minor tolerance in the torque value was also accounted due to frictional effects and power losses, since there may be current losses when the motors are used in the prototype. Motor torque outputs are selected such that they decrease subsequently as we move from the base joint to the end effector.

Upon testing the prototype, the robot followed desired trajectory by both methods of control; pre-programmed and joystick control. The motion was recorded as smooth and the structure was free of any wobble during operation. The links moved sufficiently freely through the use of bearings. The motors delivered torque as expected and the power supply was able to power the whole prototype completely.

6.2 Recommendations

Being such a versatile machine, the articulated robot arm can be used for dozens of applications. Even as a paint robot, there is room for innovation which only knows the bounds as one's imagination. The prototype can be further improved in many ways:

1) Installation of a 3D camera near the end effector. A 3D camera will be able to scan the object in front of the robot and model a profile of the surface of the target object in to the program and a program can be fed into the microprocessor to enable the robot to develop an optimal trajectory on its own and follow it to paint the target object.
2) A laser scanner will enable the robot to sense the distance and angle of the target surface and hence enable the robot to reorient the end effector on its own, resulting in efficient paint application.
3) A Graphic User Interface (GUI) can easily be developed in MATLAB and certain trajectories be developed and fed in to the microcontroller program, so the use may be able to select the desired trajectory motion of the robot arm depending upon the

application. This will particularly be useful in a paint shop where a few discrete shapes of objects are painted and hence the ideal trajectories to paint such objects can be fed in to the program and called upon as need.

4) A control system can be developed so as to control the angular velocities of the various joints during operation, and a separate control mechanism to control the flowrate of the paint. Such control may be offered through a knob, a slider bar, or through an application installed in a PC or even a smartphone. This would be particularly useful in painting complex shapes, where the robot arm has to maneuver acute turns while maintaining optimal paint deposition rates.
5) An additional axis can also be added to the robot arm. This axis would allow the robot to translate in a direction as a whole unit. Hence, the seventh incorporated axis will allow the robot arm to access the nose of the car as well as the trunk of the same car in a paint shop, therefore eliminating the need for multiple robots painting the same automobile. In such an arrangement, even a single robot can paint a whole automobile on its own, it two additional mutually perpendicular translational axes are incorporated into the arrangement, so as to allow the robot to move back and forth and sideways, all the while performing the standard motions of the six axes.

REFERENCES

[1] Akafuah, et al. *Evolution of the automotive body coating process,* 2016.

[2] Martin D. Rola. *Robotic Painting- A new phase in the robotic paint application,* 2007.

[3] Johanna Wallen. *The history of the industrial robot, 2008.*

[4] Gunnar S. Bolmsjo. *Industriell robotteknik,* 1992.

[5] *Automotive paint systems,* 2009.

[6] Occupational exposure as a painter, *IARC Monograph Vol 100F,* 2010.

[7] Mark Freels, *Robotic paint automation for smaller industrial operations,* 2008.

[8] *Advanced Micro-controls, Inc.*

[9] *Material handling robots,* 2019.

[10] Bennet Brumson, *Robotic material handling*, 2012.

[11] *Robotics and automated assembly relieve repetitive strain in workers*, 2016.

[12] Ray Marquiss, *Indutrial robots Valin Corporation¸*2018.

[13] Paint robots in the automotive industry – process and cost optimization, ABB Review 4/1996

[14] Arun Gowtham Gudla (2012), A methodology to determine the functional workspace of a 6R robot using forward kinematics, Electronic theses and desertations, 4809

[15] Fredrik Nordgren and Maria Nyquist (2006), FE-modelling of PC/ABS - experimental tests and simulations, 06/5123-183

[16] Dimensions of Denso V60. (2019). Retrieved from: https://www.densoroboticseurope.com/sites/default/files/image/Products/dimensions/vs50-60-dimensions

[17] Mid-size paint robot FANUC P-40iA. (2016). Retrieved from: https://www.fanuc.eu/ru/en/robots/robot-filter-page/paint-series/p-40ia

[18] Mohammed Almaged, (2017), Forward and Inverse Kinematic Analysis and Validation of the ABB IRB 140 Industrial Robot, International Journal Of Electronics, Mechanical And Mechatronics Engineering Vol.7 Num.2 - 2017 (1383-1401)

[19] Zennir Yousuf, Makbouche Adel, Souames Hamza, (2015), Dynamic And Kinematic Simulation Of Kawasaki Manipulator Industrial Robot Using Solidoworks And Matlab Simmechanics, 20-2101

[20] Robert L. Williams II, (1999), Inverse Kinematics and Singularities Of Manipulators With Offset Wrist, IASTED International Journal of Robotics and Automation Vol. 14, No. 1, pp. 1-8

[21] Rosheim, M.E., 1987, "Singularity-Free Hollow Spray Painting Wrists", Robots 11 Conference Proceedings RI/SME, Chicago, IL, pp. 13.7-13.28

[22] Norbert Priotrwoski, Adam Barylski, (2014), Modelling of a 6DOF manipulator in MATLAB software, Archives of mechanical engineering technology and automation, 2014, Vol. 34, no. 3

[23] P Surendernath, 2 K.Nagaraja Rao, (2015), Modelling Of A Robotic Arm Using Solid Works, International Journal of Research, Vol. 4, Issue 5

[24] ASM Materials Datasheet – Aluminium 6061-T6; 6061-T651. (2018)

Retrieved from: http://asm.matweb.com/search/SpecificMaterial.asp?bassnum=MA6061T6

[25] Characteristic curve of NEMA -17 Stepper. (2018).Retrieved from: https://motion.schneider-electric.com/hybrid-stepper-motor/m-17-nema-17-1-5-1-8-stepper-motor/

[26]Zongxing Lu Chunguang Xu, Qinxue Pan, (2015), Inverse Kinematic Analysis and Evaluation of a Robot for Nondestructive Testing Application, 18-3633/1

[27] Mohammed Almaged1, (2016), Forward and Inverse Kinematic Analysis and Validation of the ABB IRB 140 Industrial Robot, 14-2364/6

[28] John. J. Craig, Introduction to Robotics

APPENDIX I

6.1 Properties of Aluminum 6061[24]

Material Behaviour	Linear Elastic	
Mechanical Properties	Average Value	Unit
Density	2700	kg/m^3
Elastic Modulus	6890	MPa
Poisson's Ratio	0.333	-
Ultimate Tensile Strength	310	MPa
Tensile Strength	241	MPa
Yield Strength	145	MPa
Fatigue Strength	965	MPa
Thermal Conductivity	154	W/(m-K)
Rockwell Hardness ($73\ ^0F$)	40	-
Izod Impact Strength, notched (23^0C)	10.5	kJ/m^2

.

6.2 Determination of the Jacobian and then its inverse [28]

To find the joint rates or angular velocities for the motors through MATLAB, following code was used

```
syms a b c d e f;
Jv2=cross(R10,D2);
omega2=R10;
T10 = [cos(a) -sin(a) 0 150; 0 0 -1 120; sin(a) cos(a) 0 0; 0
0 0 1];
T21=[cos(b) -sin(b) 0 350; sin(b) cos(b) 0 0; 0 0 1 0;0 0 0
1];
T32=[cos(c) -sin(c) 0 65; 0 0 -1 60; sin(c) cos(c) 0 0;0 0 0
1];
T43=[cos(d) -sin(d) 0 0;0 0 1 270; -sin(d) -cos(d) 0 0; 0 0 0
1];
T54=[cos(e) -sin(e) 0 0; 0 0 -1 0; sin(e) cos(e) 0 0 ;0 0 0
1];
T65=[cos(f) -sin(f) 0 0; sin(f) cos(f) 0 0; 0 0 1 100;0 0 0
1];
T20=T10*T21;
T30=T20*T32;
T40=T30*T43;
T50=T40*T54;
T60=T50*T65;
d10=[T10(1,4); T10(2,4); T10(3,4)];
D10=simplify(d10);
d20=[T20(1,4); T20(2,4); T20(3,4)];
D20=simplify(d20);
d30=[T30(1,4);T30(2,4);T30(3,4)];
D30=simplify(d30);
d40=[T40(1,4); T40(2,4); T40(3,4)];
D40=simplify(d40);
d50=[T50(1,4); T50(2,4); T50(3,4)];
D50=simplify(d50);
```

```
d60=[T60(1,4); T60(2,4); T60(3,4)];
D60=simplify(d60);
D1=D60;
D2=simplify(D60-D10);
D3=simplify(D60-D20);
D4=simplify(D60-D30);
D5=simplify(D60-D40);
D6=simplify(D60-D50);
R00=[0;0;1];
R10=[ T10(1,3);  T10(2,3);  T10(3,3)];
R20=[ T20(1,3);  T20(2,3);  T20(3,3)];
R30=[ T30(1,3);  T30(2,3);  T30(3,3)];
R40=[ T40(1,3);  T40(2,3);  T40(3,3)];
R50=[ T50(1,3);  T50(2,3);  T50(3,3)];
R60=[ T60(1,3);  T60(2,3);  T60(3,3)];
% the Jacobian components for all 6 joints
% these are all 3*1 vectors
Jv1=cross(R00,D1);
omega1=R00;
Jv3=cross(R20,D3);
omega3=R20;
Jv4=cross(R30,D4);
omega4=R30;
Jv5=cross(R40,D5);
omega5=R40;
Jv6=cross(R50,D6);
omega6=R50;
jacobian=[Jv1 Jv2 Jv3 Jv4 Jv5 Jv6; omega1 omega2 omega3 omega4
omega5 omega6 ];
J = inv(jacobian);
```